

Automated tube potential selection for standard chest and abdominal CT in follow-up patients with testicular cancer: comparison with fixed tube potential

Ralph Gnannt · Anna Winklehner · Daniel Eberli ·
Alexander Knuth · Thomas Frauenfelder ·
Hatem Alkadhi

Received: 7 February 2012 / Revised: 21 February 2012 / Accepted: 24 February 2012 / Published online: 2 May 2012
© European Society of Radiology 2012

Abstract

Objective To evaluate prospectively, in patients with testicular cancer, the radiation dose-saving potential and image quality of contrast-enhanced chest and abdominal CT with automated tube potential selection.

Methods Forty consecutive patients with testicular cancer underwent contrast-enhanced arterio-venous chest and portal-venous abdominal CT with automated tube potential selection (protocol B; tube potential 80–140 kVp), which is based on the attenuation of the CT topogram. All had a first CT at 120 kVp (protocol A) using the same 64-section CT machine and similar settings. Image quality was assessed; dose information ($CTDI_{vol}$) was noted.

Results Image noise and attenuation in the liver and spleen were significantly higher for protocol B ($P < 0.05$ each), whereas attenuation in the deltoid and erector spinae muscles was similar. In protocol B, tube potential was reduced to 100 kVp in 18 chest and 33 abdominal examinations, and to 80 kVp in 5 abdominal CT examinations; it increased to 140 kVp in one patient. Image quality of examinations using both CT protocols was rated as diagnostic.

$CTDI_{vol}$ was significantly lower for protocol B compared to protocol A (reduction by 12%, $P < 0.01$).

Conclusion In patients with testicular cancer, radiation dose of chest and abdominal CT can be reduced with automated tube potential selection, while image quality is preserved.

Keywords Computed tomography · Radiation dose · Tube potential · Testicular cancer · Image quality

Introduction

Testicular cancer is the most common tumor in young men aged 20 to 35 years, with a 61% increase in incidence from 1973 to 2003 [1]. Most testicular cancers are germ cell tumors (GCT), which are classified for treatment purposes into two groups: seminoma and non-seminoma germ cell tumors (NSGCT). Regardless of the histopathological subtype or stage, cure can be expected in more than 95% of cases, even with metastatic disease at presentation [2]. Most important factors for this high cure rate are careful staging at the time of diagnosis as well as early treatment including surgery and chemotherapy, either with or without radiotherapy [3]. Lifelong cure rates are high, but since there is a risk for relapse close surveillance remains inevitable.

Taking into consideration the potential cure and relative young age of patients with testicular cancer, particular care should be taken when imaging this patient population regarding the applied cumulative radiation dose of repetitive chest and abdominal CT. For example for the follow-up of seminomas treated with orchiectomy without adjuvant therapy, international guidelines propose for stage I tumors at least ten abdominal and five chest CT scans within the first 5 years. Beyond 5 years of surveillance post-treatment no

R. Gnannt · A. Winklehner · T. Frauenfelder · H. Alkadhi (✉)
Institute of Diagnostic and Interventional Radiology, University
Hospital Zurich,
Raemistrasse 100,
CH-8091 Zurich, Switzerland
e-mail: hatem.alkadhi@usz.ch

D. Eberli
Clinic for Urology, University Hospital Zurich,
Zurich, Switzerland

A. Knuth
Clinic for Oncology, University Hospital Zurich,
Zurich, Switzerland

further CT scans are recommended, except in NSGCT with a disseminated disease at first presentation where a surveillance period of 10 years is recommended [4].

Ionizing radiation from CT imaging is assumed to increase the lifetime attributable risk for developing cancer [5]. This holds particularly true for patients undergoing repetitive CT studies. Sodickson et al. [6] reported that 33% of their patients undergoing CT imaging in their hospital had more than five lifetime CT examinations and 5% of patients having undergone at least 22 CT examinations, resulting in a cumulative effective radiation dose of more than 100 mSv in 15% of the population. At this level of radiation exposure, there is convincing epidemiologic evidence of increased cancer risk [7].

Several techniques exist to reduce the radiation exposure of chest and abdominal CT studies. The most widely applied option is automated tube current modulation (ATCM), enabling the adjustment of the tube current to the attenuation of the body region with the aim of maintaining constant image quality [8]. Another approach is lowering of the tube potential from the standard 120 kVp to 100 kVp or even 80 kVp, because the radiation dose roughly changes with the square of the tube potential [9]. The downside of low tube potential CT, however, is the nonlinear increase in image noise, necessitating adjustment of the tube current in order to maintain a constant image quality.

Very recently, a new algorithm was developed that automatically selects the tube potential depending on the individual patients' attenuation profile from the CT topogram and on the diagnostic task at hand. A preliminary study indicated that this algorithm could lower the radiation dose of body CT angiography studies by up to 25% as compared to the use of a standard 120 kVp protocol, however, no patient group was available for comparison in that study [10]. In addition, the effect of this algorithm on standard contrast-enhanced chest and abdominal CT has not been investigated so far.

The purpose of this study was to assess prospectively, in patients with testicular cancer, the radiation dose-saving potential and image quality of follow-up chest and abdominal CT when using the automated tube potential selection. Our hypothesis was that use of the algorithm would result in a reduction in radiation dose while image quality would be preserved, thus being a valuable option for use in CT studies for this indication.

Materials and methods

Study population

Between January and October 2011, 47 patients who were referred for chest and abdominal CT in our imaging

department were screened for possible study inclusion. Patients were included if a previous chest and abdominal CT study, acquired at our institution, using the same CT machine and the same reference tube current-time product was available for comparison. Patients were excluded if previous imaging was not performed with the standard tube potential of 120 kVp ($n=1$), or no previous complete chest and abdominal CT examination was available ($n=6$).

Further general exclusion criteria for contrast-enhanced CT included nephropathy [defined as an estimated glomerular filtration rate <60 mL/min, ($n=0$)] untreated hyperthyroidism ($n=0$), and known hypersensitivity to iodine-containing contrast media ($n=0$). Thus, a total of 40 patients [mean age 38 ± 7.8 years, age range 18–56 years; body mass index (BMI) 25.6 ± 3.9 kg/m², BMI range: 18.8–39.6 kg/m²] were finally included in the study.

Institutional review board approval was obtained, and written informed consent was obtained from all patients.

Patient anthropometrics

The anteroposterior and lateral diameters were measured in each patient in both scans at the level of the pulmonary trunk (for the chest) and at the level of the celiac trunk (for the abdomen) by a radiologist who was not involved in further readout. In addition, body weight and body height were noted in each patient at the time of CT for both scans, for calculating the BMI.

CT data acquisition

All CT studies were performed on a 64-section CT machine (Definition AS, software package SOMARIS 7, VA40, Siemens Healthcare). In each patient and in each CT protocol, 100 mL of iopromide (Ultravist 300, 300 mg/mL, Bayer) was injected at a flow rate of 2.6 mL/s followed by 40 mL saline solution at the same flow rate. Chest CT data acquisition in a mixed arterio-venous phase was initiated using bolus tracking with a delay of 25 s after an attenuation threshold of 100 Hounsfield units (HU) was reached in a region of interest (ROI) set in the descending aorta. After an additional delay of 40 s, abdominal CT data acquisition was started in the portal-venous phase of enhancement.

The first chest and abdominal CT scan was performed with a fixed tube potential of 120 kVp (protocol A), whereas the second CT scan was performed using automated tube potential selection (protocol B). For both protocols, ATCM (CareDose4D, Siemens) was used, with a reference tube current-time product of 110 ref.mAs for the chest and 210 ref.mAs for the abdomen. These reference tube current settings represent the default settings from the vendor. The other CT parameters were kept constant: detector collimation 32×0.6 mm; slice

collimation 64×0.6 mm by means of a z-flying focal spot; pitch, 1.2; and rotation time, 0.33 s.

Chest images were reconstructed using a sharp-edged tissue convolution kernel (B60f) and abdominal images with a medium-smooth soft tissue convolution kernel (B30f) at a slice thickness of 2 mm and increment of 1.7 mm.

Automated tube potential selection algorithm

The automated tube potential selection algorithm (CarekV, Siemens Healthcare) presented herein represents a software that aims at an individual optimization of both tube potential and tube current for each scan, based on patient attenuation measured in the CT topogram and the selected diagnostic task. A previous feasibility study described the method in detail [10]. In brief, the algorithm calculates the required tube current to reach a user-defined image quality according to the patient's attenuation along the z-axis obtained from the CT topogram. If this can be achieved at a low tube potential (e.g., 80 kVp), the scan is performed. If the required tube current at any location of the CT topogram exceeds the system limits, the software switches to the next higher tube potential (100, 120, or 140 kVp) and the calculation is repeated.

CT image analysis

Subjective image quality

Two independent radiologists (with 4 years of experience in body radiology each) assessed the overall image quality on the transverse CT images of the chest and abdomen. The CT datasets were anonymized, randomized and the readers were blinded to the acquisition parameters. Before beginning the assessment, both readers were instructed on the criteria of image grading and assessed three test cases together that were not included in the study.

The images of protocols A and B were analyzed qualitatively by the two readers, by rating overall image quality using a five-point scale: score 1=excellent; score 2=good; score 3=mild impairment; score 4=moderate impairment, still interpretable; and score 5=severe impairment, nondiagnostic.

Then, the same two radiologists evaluated the visually sharp reproduction of four anatomic structures in the chest and abdomen each as described in the European Guidelines on Quality Criteria for CT, using a dichotomous scale (1=good to excellent; 2=moderate). Anatomic structures for the chest were carina and lymph node area, esophagus, large and medium sized pulmonary vessels, and lung parenchyma. Anatomic structures for the abdomen were perivascular retroperitoneal space, kidneys and proximal ureter, lymph nodes smaller than 15 mm, and liver parenchyma and intrahepatic vessels [11].

The readers could individually adjust window center and width for optimal image impression.

Objective image quality

Quantitative image analysis was performed by two other independent and blinded radiologists (with 7 and 8 years of experience in body radiology, respectively) not involved in the readout described above.

Image noise was defined as the standard deviation of attenuation measured in the air of the carina (N_{chest}) and in the air ventral to the abdomen on the level of the celiac trunk (N_{abd}) [12].

Attenuation was measured in the following anatomic structures: in the right deltoid muscle (ROI_{DM}), in liver segment VIII ($\text{ROI}_{\text{LSVIII}}$), in the lower pole of the spleen ($\text{ROI}_{\text{spleen}}$), and in the left erector spinae muscle at the level of L4 (ROI_{ES}).

In the chest, the signal-to-noise ratio (SNR) was calculated in the deltoid muscle ($\text{SNR}_{\text{DM}} = \text{ROI}_{\text{DM}} / N_{\text{chest}}$). In the abdomen, we calculated the SNR in liver segment VIII ($\text{SNR}_{\text{LSVIII}} = \text{ROI}_{\text{LSVIII}} / N_{\text{abd}}$) and in the spleen ($\text{SNR}_{\text{spleen}} = \text{ROI}_{\text{spleen}} / N_{\text{abd}}$). In addition, we calculated the SNR for the erector spinae muscle ($\text{SNR}_{\text{ES}} = \text{ROI}_{\text{ES}} / N_{\text{abd}}$).

The contrast-to-noise ratio (CNR) was calculated in the liver and spleen as follows: $\text{CNR}_{\text{LSVIII}} = (\text{ROI}_{\text{LSVIII}} - \text{ROI}_{\text{ES}}) / N_{\text{abd}}$ and $\text{CNR}_{\text{spleen}} = (\text{ROI}_{\text{spleen}} - \text{ROI}_{\text{ES}}) / N_{\text{abd}}$.

Radiation dose estimation

The effective radiation dose delivered at chest and abdominal CT was calculated applying a method proposed by the European Working Group for Guidelines on Quality Criteria for CT [13]. The volume CT dose index (CTDI_{vol}) and dose-length product (DLP) were obtained from the patient protocol that summarized the individual radiation exposure parameters of each CT scan. Percentage dose reduction was calculated as $[\text{CTDI}_{\text{vol}}(\text{protocol A}) - \text{CTDI}_{\text{vol}}(\text{protocol B})] \times 100 / \text{CTDI}_{\text{vol}}(\text{protocol A})$. Effective radiation doses were calculated by multiplying the DLP with the conversion coefficient $k=0.014$ for the chest and the coefficient $k=0.015$ for the abdomen [14].

Statistical analysis

Continuous variables are expressed as means \pm standard deviations (range) or as medians and ranges. Categorical variables are expressed as frequencies or percentages. Inter-reader agreement was assessed with Cohen's kappa (κ) statistics ($\kappa > 0.81$: excellent agreement; $\kappa = 0.61$ – 0.80 : good agreement; $\kappa = 0.41$ – 0.60 : moderate agreement; $\kappa = 0.21$ – 0.40 : fair agreement; and $\kappa < 0.20$: poor agreement) for subjective image quality scores and with Pearson's correlation for

quantitative parameters. The relationship between BMI and automated kV selection was assessed with the Spearman rank order correlation test. Differences in image quality scores between protocol A and B were assessed using the Wilcoxon signed ranks test. Mean effective tube current, attenuation, contrast, noise, SNR, CNR, patient diameter, and radiation dose were compared between protocol A and B using paired samples *t*-tests or the Wilcoxon signed ranks test, depending on normality testing with the Kolmogorov-Smirnov test.

All statistical analyses were performed using commercially available software (SPSS, release 19, Chicago, IL). Two-sided *P*-values < 0.05 were considered to be statistically significant.

Results

Patients

All 40 patients had histologically proven GCT of the testis, including 27/40 (67.5%) pure seminoma and 13/40 (32.5%) mixed embryonal carcinoma, teratoma, and seminoma. Out of the 27 seminomas, 22 (81%) were stage I, 4 (15%) were stage II, and 1 (4%) was stage III. Of the mixed carcinomas, 8 of 13 (62%) were stage I, 3 (23%) were stage II, and 2 (15%) were stage III tumors. All patients with stage II and III tumors received chemotherapy after orchiectomy except one patient (stage II) who refused adjuvant therapy. Eighteen of 30 (60%) patients with stage I tumors received chemotherapy after surgery. There were two mixed tumors that relapsed but were successfully treated with chemotherapy. Both of these patients had no adjuvant therapy.

The median time interval for all 40 patients between orchiectomy and protocol B was 797 days (mean 953 ± 629 days, range 78–2,657 days). In this time interval, a total of 137 chest and 145 abdominal CT scans were performed on these 40 patients, resulting in an average of 3.4 ± 1.8 (median 3, range 1–9) chest and 3.6 ± 1.9 (median 4, range 1–9) abdominal CT scans per patient.

Patient anthropomorphics

Protocols A and B were performed within a median time interval of 365 days (mean 422 ± 338 days, range 53–1,112 days). There were no significant differences in patient size between the two protocols for the anteroposterior (protocol A: 22.8 ± 2.2 cm vs. protocol B: 22.8 ± 2.2 cm; *P* = 0.98) and the lateral diameter (A: 38.7 ± 2.6 cm vs. B: 38.8 ± 2.5 cm; *P* = 0.64) of the chest. There were also no significant differences between protocols in patient size for the anteroposterior (protocol A: 22.8 ± 3.6 cm vs. protocol B: 23.0 ± 4.0 cm; *P* = 0.48) and lateral diameter (protocol A: 33.1 ±

4.1 cm vs. protocol B: 33.6 ± 3.9 cm; *P* = 0.15) of the abdomen. The same holds true for the BMI of the patients, which were similar between protocols (protocol A: 25.3 ± 4.0 kg/m² vs. protocol B: 25.6 ± 3.9 kg/m², range 18.8–39.6 kg/m²; *P* = 0.54).

A significant correlation was found between the lateral and the anteroposterior diameter of the thorax and the automated kVp selection for chest CT (*r* = 0.61, *P* < 0.001 and *r* = 0.33, *P* < 0.05, respectively). Similarly, significant correlations were found between the anteroposterior and lateral diameter of the abdomen with the automated kVp selection for abdominal CT (*r* = 0.60, *P* < 0.001 and *r* = 0.54, *P* < 0.001, respectively).

Also, a significant correlation was found between the BMI and the automated kVp selection for the chest (*r* = 0.48, *P* < 0.001) and for the abdomen (*r* = 0.39, *P* < 0.05) (Fig. 3).

CT image analysis

Subjective image quality

The mean image quality score for reader 1 was 1.53 ± 0.64 (range score 1–3) in protocol A and 1.58 ± 0.71 (range score 1–3) in protocol B (*P* = 0.64) (Fig. 1). The mean image quality score for reader 2 was 1.65 ± 0.73 in protocol A and 1.73 ± 0.75 in protocol B (*P* = 0.50). None of the readers rated image quality with score 4 (moderate impairment) or score 5 (severe impairment, nondiagnostic). The interobserver agreement was good for both protocols (A; κ = 0.76) and (B; κ = 0.78).

Visually sharp reproductions of the liver parenchyma and intrahepatic vessels were rated insufficient in one image set from protocol B by both readers (Fig. 2). Both readers rated all other anatomic structures in the chest and abdomen in both scans as being visually sharp reproductions.

Objective image quality

Objective image quality parameters for protocols A and B showed a high correlation between readers (all *r* > 0.81). Therefore, the mean from both readers was used for further analysis.

Image noise was significantly higher in protocol B as compared to protocol A for the chest and the abdomen. The attenuation was significantly higher for protocol B compared to protocol A for the liver and spleen, whereas attenuation was similar in the deltoid and erector spinae muscles (Table 1).

There was no significant difference in SNR for the liver (*P* = 0.06) and spleen (*P* = 0.07) between protocols. For muscle tissue the SNR was significantly higher in protocol A compared to protocol B (*P* < 0.05, see Table 1).

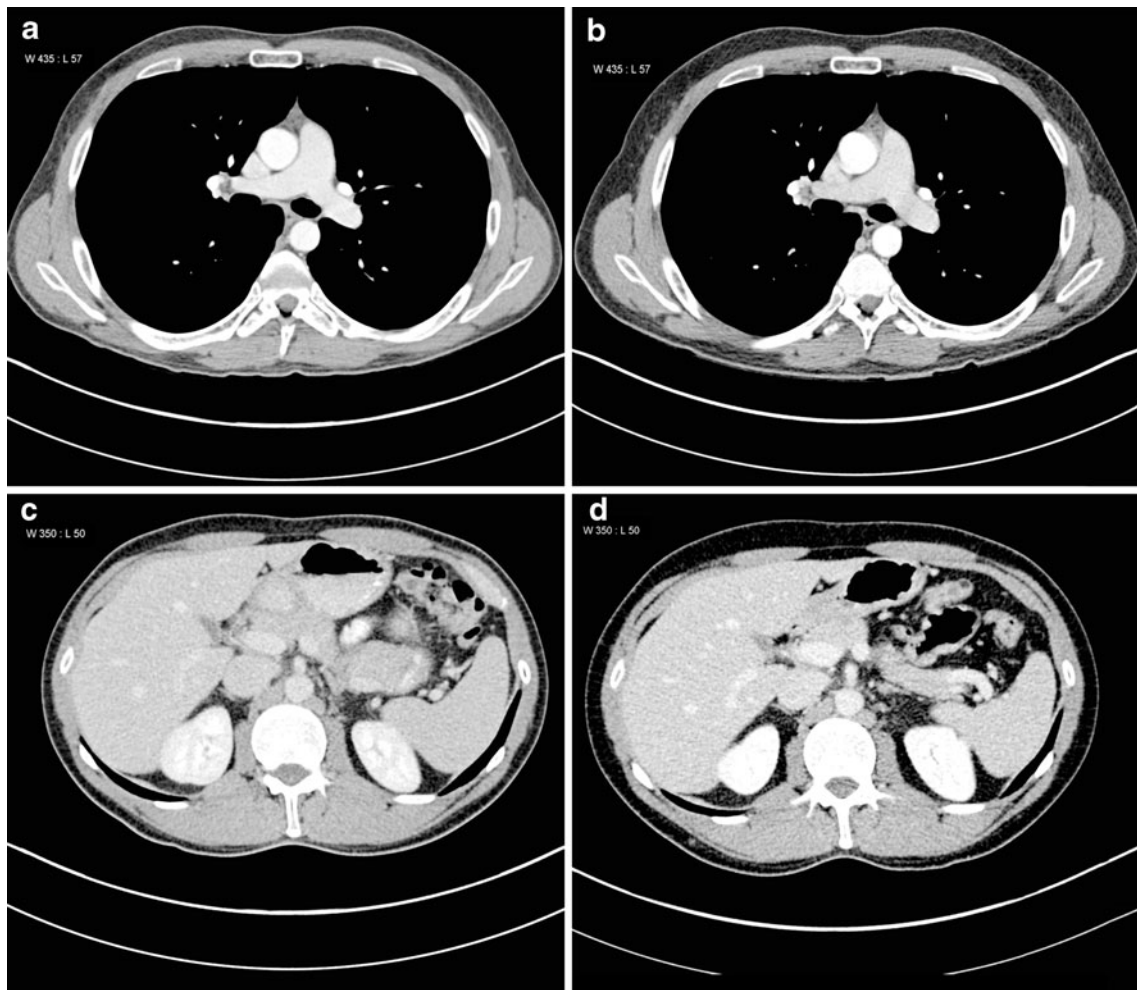


Fig. 1 Arterio-venous chest and portal-venous abdominal CT images in a 42-year-old male patient with a testicular seminoma scanned at 120 kVp (99 eff.mAs) for the chest (a) and 120 kVp (132 eff.mAs) for the abdomen (c), as compared to 100 kVp (131 eff.mAs) for the chest

(b) and 80 kVp (405 eff.mAs) for the abdomen (d) with automated tube potential selection. Image quality of both CT studies was rated excellent (score 1) by both readers. Radiation dose for the chest CT was reduced by 27% and for the abdomen by 18%

Similar to the SNR, there was no significant difference in the CNR in the liver ($P=0.66$) and spleen ($P=0.11$, see Table 1) between protocols.

Radiation dose estimation

For chest CT, automated tube potential selection (protocol B) led to a reduction to 100 kVp in 18/40 (45.0%) patients, whereas tube potential remained at 120 kVp in 21/40 (52.5%). In one patient (2.5%) tube potential increased to 140 kVp.

For abdominal CT, automated tube potential selection (protocol B) led to a reduction to 80 kVp in 5/40 (12.5%) and to 100 kVp in 34/40 (85%) patients, whereas in 1 patient (2.5%) tube potential increased to 140 kVp (the same patient in whom tube potential increased for chest CT). Using the algorithm, no patient's abdomen was scanned at a tube potential of 120 kVp.

Effective mAs was significantly higher in protocol B (chest: 143.1 ± 18.4 eff.mAs, abdomen: 308.4 ± 71.3 eff.mAs) compared to protocol A (chest: 136.4 ± 26.5 eff.mAs, $P < 0.001$; abdomen: 206.2 ± 55.3 eff.mAs, $P < 0.001$).

CTDI_{vol} and DLP were significantly lower for protocol B (chest: 8.6 ± 2.8 mGy, 324.9 ± 100.8 mGy·cm; abdomen: 13.0 ± 4.8 mGy, 636.9 ± 260.5 mGy·cm) compared to protocol A (chest: 9.8 ± 1.8 mGy, 379.5 ± 64.4 mGy·cm; abdomen: 14.8 ± 3.8 mGy, 759.6 ± 223.8 mGy·cm; each $P < 0.01$). The percentage dose reduction for both chest CT and abdominal CT was 12% on average. When including only those patients in whom the automated tube potential selection reduced the kVp, average radiation dose reduction was 44% for chest and 17% for abdominal CT (see Table 2).

Using the conversion coefficients for the chest and abdomen, estimated effective radiation dose with use of automated tube potential selection for chest CT was 4.9 mSv, and estimated effective radiation dose for abdominal CT was 9.6 mSv.

Table 2 Radiation dose estimates with the automated tube potential selection algorithm (protocol B)

Protocol B	kVp	Number	Mean±SD CTDI _{vol} (mGy)	Overall CTDI _{vol} (mGy)
Chest	140	1	19.18	8.65±2.83
	120	21	10.0±1.72	
	100	18	6.3±0.51	
	80	0	-	
Abdomen	140	1	37.54	12.96±4.82
	120	0	-	
	100	34	12.9±2.46	
	80	5	8.47±0.6	

CTDI_{vol} Computed tomography dose index, SD standard deviation

noise [15–17]. In this study, we introduce a new option for radiation dose reduction, i.e., automated tube potential selection. This algorithm aims at an individual optimization of tube potential in combination with tube current in each study, based on the patient's attenuation obtained from the CT topogram and the diagnostic task at hand. While a previous preliminary study suggested a potential dose reduction of 25% in body CT angiography studies [10], our results demonstrate that this algorithm can also be used in standard contrast-enhanced CT studies of the chest and abdomen resulting in a reduction of radiation dose by 12% for both chest and abdominal CT, while diagnostic image quality is maintained.

Lowering of the tube potential leads to lower photon penetration and corresponding increase in image noise. When lowering the tube potential, tube current should be increased to compensate for this increase in noise [18]. Previous studies employed different measures and thresholds for reducing tube potential in CT angiography [19, 20]. Some authors used the patients' BMI as a measure with a reduction of tube potential below 25 kg/m². Other authors used body weight as the measure and reduced the tube potential below 70 kg [19]. We assume that because of these various approaches, together with the need for adjusting the tube current accordingly, the individual and manual lowering and optimizing of the tube potential is rather rarely used in daily clinical routine. An algorithm such as the one presented herein might represent a solution to this dilemma by automatically selecting the tube potential based on the individual attenuation of the patient in the topogram and the individual diagnostic task.

Most previous studies have addressed the use of low tube potential for CT angiography [21]. This is explained by the fact that lowering the tube potential in body CTA has the advantage of providing higher attenuation of iodinated contrast media as a result of the greater photoelectric effect and decreased Compton scattering [22]. The nearer the tube potential approaches the k-edge of iodine at 33 keV, the

greater the attenuation of the contrast media. As a matter of fact, reducing the tube potential to 100 kVp or even 80 kVp in CT angiography results in contrast-to-noise ratio levels similar to those for 120 kVp, despite the higher image noise, while significantly reducing radiation dose [23, 24]. Interestingly, use of low tube potential for standard contrast-enhanced CT has been the subject of only a few studies, all focusing on the upper abdomen [25, 26]. For example Marin and coworkers evaluated the use of low tube potential CT in patients with malignant hypervascular liver tumors. The authors showed an increase in image noise, while the contrast-to-noise ratio and lesion conspicuity were higher at a low tube potential. Most importantly, the low tube potential protocol was associated with a significantly lower effective dose [26]. In our study, we also found a higher image noise in the chest and abdomen. In the normal liver and spleen, attenuation was significantly higher at lower tube potentials. In contrast, attenuation was similar in the deltoid and erector spinae muscle between the protocols. This is most probably explained by the iodine content in the liver and spleen scanned in the portal-venous phase of enhancement, whereas the attenuation of the muscles—being only slightly perfused with blood and hence, iodine—remained at a similar level. Both the SNR and the CNR were not significantly different for the 120 kVp protocol as compared to the low tube potential protocol in the liver and spleen. Thus, it appears that with low kVp scanning, the increase in attenuation in these organs matched the corresponding increase in image mottle, similar to previous results in body CT angiography [21]. In contrast, the lack of increase in attenuation in the muscles did not outweigh the increase in image noise, leading to lower SNR in these areas. Most importantly, the overall image quality of images generated with automated tube potential selection was rated as being diagnostic by both readers in all patients, including a visually sharp reproduction of various anatomic structures in the chest and abdomen. This is also reflected by the fact that all CT studies could be readily used for daily routine diagnostics.

The algorithm tested herein lowered the tube potential to 100 kVp for chest CT in 45% of the patients and increased the tube potential in one patient to 140 kVp. Tube potential reduction was not reduced to 80 kVp for any chest CT. The most likely explanation for that is the algorithm itself, which requires higher tube current at lower tube potentials. When the attenuation based on the CT-acquired digital radiograph is high, requiring a tube current that exceeds the system limits of the tube, the algorithm switches to the next higher tube potential, until the required tube current can be provided. We might speculate that in our patients, the relatively high attenuation at the level of the shoulders necessitated a tube current that could not be provided by the tube at 80 kVp; therefore, the next higher tube potential was chosen by the algorithm.

For abdominal CT, the algorithm lowered tube potential to 80 kVp in 12.5% and to 100 kVp in 85% of patients, whereas in one patient tube potential increased to 140 kVp. The patient in whom this increase in tube potential occurred had a BMI of 39.6 kg/m². Interestingly, the selected tube voltage showed significant correlations to patient anthropomorphics including the BMI and chest and abdominal body diameters. This indicates that the parameters used by the algorithm represent a surrogate for patient habitus. Nevertheless, there was a considerable overlap of these parameters and the selected kVp, as can be seen in Fig. 3 for the BMI and patients scanned at 100 and 120 kVp for the chest, and patients scanned at 80 and 100 kVp for the abdomen. This may be explained by the fact that automated tube potential selection is based on various factors beyond the patient's BMI alone, including the individual patient's attenuation of the topogram, the body region imaged, and the clinical task at hand.

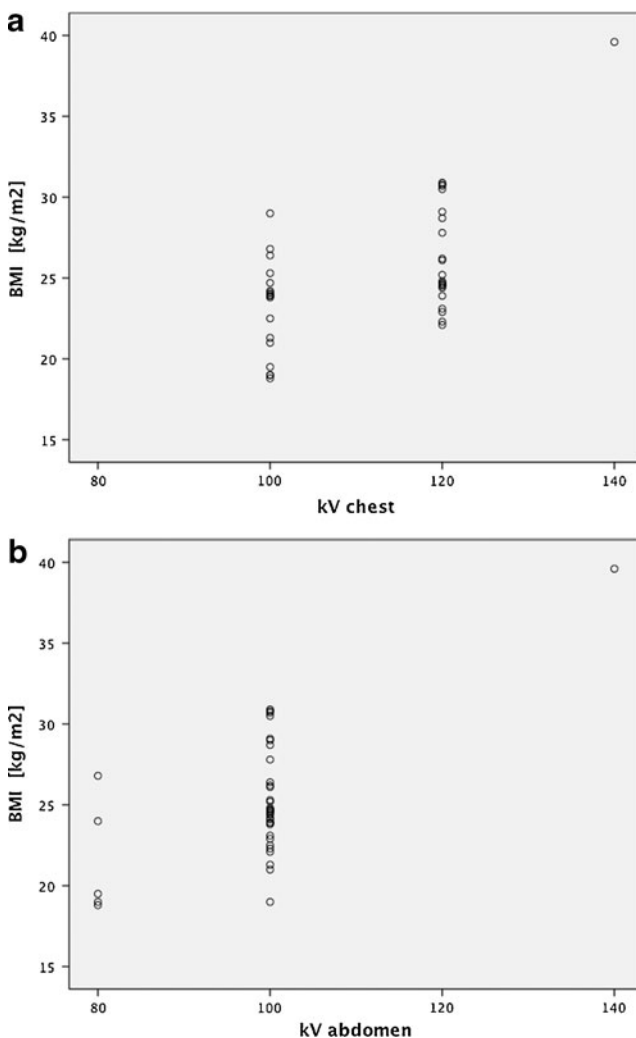


Fig. 3 Scatter plots demonstrating the correlation between the body mass index (BMI) and the automatically selected tube potential for chest ($r=0.48$; $P<0.001$) (a) and abdominal CT ($r=0.39$; $P<0.05$) (b)

Our study indicates that radiation dose of standard, contrast-enhanced chest and abdominal CT studies can be lowered by an average of 12% for the chest and 12% for the abdomen, without losing the diagnostic quality of the examination. When including only those patients in whom the algorithm reduced the kVp settings, radiation dose was reduced by 44% for chest and 17% for abdominal CT. Still this value is below the average 25% dose reduction reported by Winklehner et al. [10] who tested the algorithm in body CT angiography. The most probable reason for this difference is the influence of the selected diagnostic task of the CT study, because the amount of required mAs adaptation in case of changed kVp depends on the respective protocol settings. In the case of a CT angiography study, a smaller increase in the mAs is required at lower tube potentials than in contrast-enhanced CT studies for parenchymal abdominal organs, since those benefit less from the higher attenuation of iodine (and therefore higher CT numbers) with lower kVp. Because these settings were defined after selecting the corresponding icon on the scanner interface, the radiation dose reductions for standard contrast-enhanced chest and abdominal CT were smaller than those previously reported for CT angiography.

Still we consider this radiation dose reduction as being relevant and fully complying with the ALARA principle. Our potentially curable patients with testicular seminoma were relatively young, thus more susceptible to ionizing radiation than an older population. In addition, these patients often undergo repetitive CT imaging for surveillance purposes. In our study, the patients had undergone a median of three chest and four abdominal CT studies since orchiectomy, thus highlighting the issue of cumulative radiation dose from repetitive CT. Most importantly, the dose reduction algorithm presented herein can be used as an adjunct to other dose-saving approaches such as ATCM, as demonstrated in this study, or with iterative reconstructions [15–17].

Some study limitations must be acknowledged. First, the number of patients included was limited. Second, the scans were performed at two distinct time points potentially allowing other factors to play a role with regard to image quality. However, we tried to hold as many parameters constant as possible, including the CT machine and the protocol parameters (except the tube potential), and we controlled for stable patient anthropomorphics over time. Finally, magnetic resonance (MR) imaging would be an alternative modality for follow-up in this patient population to CT. However, current data on MR imaging in these patients are limited [27], and most recent guidelines still propose CT as the method of choice [4].

In conclusion, our study indicates that in patients with testicular cancer, use of an automated tube potential selection algorithm results in diagnostic image quality, while radiation

dose is reduced by around 12% for chest and 12% for abdominal CT. Thus, use of such algorithms can be recommended for reducing the cumulative radiation doses from repetitive CT in the relatively young and potentially curable patients.

References

- Shah MN, Devesa SS, Zhu K, McGlynn KA (2007) Trends in testicular germ cell tumours by ethnic group in the United States. *Int J Androl* 30:206–213, discussion 213–204
- Huddart RA, Birtle AJ (2005) Recent advances in the treatment of testicular cancer. *Expert Rev Anticancer Ther* 5:123–138
- Albers P, Albrecht W, Algaba F et al (2005) Guidelines on testicular cancer. *Eur Urol* 48:885–894
- Schmoll HJ, Jordan K, Huddart R et al (2010) Testicular seminoma: ESMO clinical practice guidelines for diagnosis, treatment and follow-up. *Ann Oncol* 21:v140–v146
- Amis ES Jr, Butler PF (2010) ACR white paper on radiation dose in medicine: three years later. *J Am Coll Radiol* 7:865–870
- Sodickson A, Baeyens PF, Andriole KP et al (2009) Recurrent CT, cumulative radiation exposure, and associated radiation-induced cancer risks from CT of adults. *Radiology* 251:175–184
- Brenner DJ, Doll R, Goodhead DT et al (2003) Cancer risks attributable to low doses of ionizing radiation: assessing what we really know. *Proc Natl Acad Sci USA* 100:13761–13766
- Kalra MK, Maher MM, Toth TL et al (2004) Techniques and applications of automatic tube current modulation for CT. *Radiology* 233:649–657
- Huda W, Scalzetti EM, Levin G (2000) Technique factors and image quality as functions of patient weight at abdominal CT. *Radiology* 217:430–435
- Winklehner A, Goetti R, Baummueller S et al (2011) Automated attenuation-based tube potential selection for thoracoabdominal computed tomography angiography: improved dose effectiveness. *Invest Radiol* 46:767–773
- Radiology DSo (1998) European guidelines on quality criteria for computed tomography. <http://www.dr.dk/guidelines/ct/quality/index.htm>
- May MS, Wust W, Brand M et al (2011) Dose reduction in abdominal computed tomography: intraindividual comparison of image quality of full-dose standard and half-dose iterative reconstructions with dual-source computed tomography. *Invest Radiol* 46:465–470
- AAPM Task Group 23 of the Diagnostic Imaging Council CT Committee (2008) The measurement, reporting, and management of radiation dose in CT. The American Association of Physicists in Medicine, College Park, MD
- Shrimpton PC, Hillier MC, Lewis MA, Dunn M (2006) National survey of doses from CT in the UK: 2003. *Br J Radiol* 79:968–980
- Pontana F, Pagniez J, Flohr T et al (2011) Chest computed tomography using iterative reconstruction vs filtered back projection (Part 1): evaluation of image noise reduction in 32 patients. *Eur Radiol* 21:627–635
- Winklehner A, Karlo C, Puipe G et al (2011) Raw data-based iterative reconstruction in body CTA: evaluation of radiation dose saving potential. *Eur Radiol* 21:2521–2526
- Mitsumori LM, Shuman WP, Busey JM, Kolokythas O, Koprowicz KM (2012) Adaptive statistical iterative reconstruction versus filtered back projection in the same patient: 64 channel liver CT image quality and patient radiation dose. *Eur Radiol* 22:138–143
- Gnannt R, Winklehner A, Goetti R, Schmidt B, Kollias S, Alkadhi H (2012) Low kilovoltage CT of the neck with 70 kVp: comparison with a standard protocol. *AJNR Am J Neuroradiol*. doi:10.3174/ajnr.A2910
- Nakayama Y, Awai K, Funama Y et al (2006) Lower tube voltage reduces contrast material and radiation doses on 16-MDCT aortography. *AJR Am J Roentgenol* 187:W490–W497
- Yu L, Li H, Fletcher JG, McCollough CH (2010) Automatic selection of tube potential for radiation dose reduction in CT: a general strategy. *Med Phys* 37:234–243
- Alkadhi H, Schindera ST (2011) State of the art low-dose CT angiography of the body. *Eur J Radiol* 80:36–40
- Leschka S, Stolzmann P, Schmid FT et al (2008) Low kilovoltage cardiac dual-source CT: attenuation, noise, and radiation dose. *Eur Radiol* 18:1809–1817
- Wintersperger B, Jakobs T, Herzog P et al (2005) Aorto-iliac multidetector-row CT angiography with low kV settings: improved vessel enhancement and simultaneous reduction of radiation dose. *Eur Radiol* 15:334–341
- Schindera ST, Graca P, Patak MA et al (2009) Thoracoabdominal-aortoiliac multidetector-row CT angiography at 80 and 100 kVp: assessment of image quality and radiation dose. *Invest Radiol* 44:650–655
- Marin D, Nelson RC, Barnhart H et al (2010) Detection of pancreatic tumors, image quality, and radiation dose during the pancreatic parenchymal phase: effect of a low-tube-voltage, high-tube-current CT technique—preliminary results. *Radiology* 256:450–459
- Marin D, Nelson RC, Samei E et al (2009) Hypervascular liver tumors: low tube voltage, high tube current multidetector CT during late hepatic arterial phase for detection—initial clinical experience. *Radiology* 251:771–779
- Hansen J, Jurik AG (2009) Diagnostic value of multislice computed tomography and magnetic resonance imaging in the diagnosis of retroperitoneal spread of testicular cancer: a literature review. *Acta Radiol* 50:1064–1070